Supporting Information

Enhanced sensitivity using MALDI imaging coupled with laser post-ionization for pharmaceutical studies

Florian P. Y. Barré[1], Martin R. L. Paine[1], Bryn Flinders[1], Adam J. Trevitt[2], Patrick D. Kelly[2], Rima Ait-Belkacem[3], João P. Garcia[4], Laura B. Creemers[4], Jonathan Stauber[3], Rob J. Vreeken[1,5], Berta Cillero-Pastor[1], Shane R. Ellis[1], Ron M. A. Heeren[1*]

[1]The Maastricht Multimodal Molecular Imaging Institute (M4I), Division of Imaging Mass Spectrometry, Maastricht University, Universiteitssingel 50, 6229 ER Maastricht, The Netherlands.

[2]School of Chemistry, University of Wollongong, Wollongong, Australia.

[3]ImaBiotech, Loos, France.

[4]University Medical Centre (UMC) Utrecht, Department of Orthopedics, Heidelberglaan 100, 3584 CX Utrecht, The Netherlands[5]Discovery Sciences, Janssen Research & Development, Beerse, Belgium.

*Corresponding author: r.heeren@maastrichtuniversity.nl

Tissue collection

Cartilage: The anonymous use of redundant tissue for research purposes is part of the standard treatment agreement with patients in the University Medical Center Utrecht and was carried out under protocol nº 15-092 of the UMCU's Review Board of the BioBank. The cartilage was obtained from an osteoarthritic patient undergoing total knee arthroplasty and rinsed with PBS containing 1% P/S. Explants from cartilage tissue (5 × 5 mm) was placed in a 24-well plate and incubated with DMEM supplemented with 10% FBS and 1% P/S. Triamcinolone acetonide (TAA) was added (43.5 ng/µl) at a total volume of 500 µL for 48 h in a humidified incubator in an environment of 5% CO_2 and 37 °C. After the incubation, cartilage chips were rinsed with ice-cold ammonium acetate buffer (150 mM, pH 7.3), snap-frozen in liquid nitrogen, and stored at -80 °C until analysis.

Liver: Janssen R&D (Beerse, Belgium) provided canine liver tissue dosed with a drug compound A at 65 mg/kg. Liver was resected, snap-frozen on aluminium foil floating on liquid nitrogen and subsequently stored at -80 °C until sectioning and analysis. For confidentiality reasons, structural information on the drug cannot be revealed and only nominal mass information can be supplied.

All tissues were sectioned at 12-µm thickness and -20 °C using a Leica cryostat (Leica Microsystems, Wetzlar, Germany) and thaw mounted onto indium tin oxide (ITO)-coated glass slides (4-8 Ω resistance, Delta Technologies, USA) and stored at -80 °C until analysis.

Mass spectrometry and laser post-ionization

A nanosecond pulsed, Nd:YAG pumped optical parametric oscillator (OPO) laser system was used for post-ionization (Ekspla NT-230, Vilnius, Lithuania). The OPO laser beam was aligned such that it was introduced parallel to and ~ 200–400 µm above the sample surface using two UV-grade fused silica mirrors and a right angled prism (Altechna, Vilnius, Lithuania). A 25.4-cm diameter, 40-cm focal length lens used was used to focus the MALDI-2 laser within the ion source above the sample surface to a final spot size of ~ 250 µm. Control over the MALDI-2 pulse energy was achieved using an

adjustable Glan-Taylor polariser (Altechna, Vilnius, Lithuania) while the emission time was recorded using a photodiode detector (DET-10A, Thor Labs, Germany) positioned behind the second mirror. This photodiode signal, and the signal provided by the internal photodiode of the ND:YLF 349-nm MALDI laser (Explorer One, Spectra Physics, Mountain View, CA, USA) were monitored using a digital oscilloscope. Both lasers were externally triggered using time-displaced signals generated with a digital pulse/delay generator (DG645, Stanford Research Systems, Sunnyvale, USA) that provided precise control over the delay time between the two laser pulses. Further experimental details can be found in reference.[1]

Tissue staining

After MSI analysis, the matrix was removed from the tissues by immersion in 70% ethanol for 5 min and the tissue rehydrated in milliQ water. The liver section was stained with hematoxylin for 3 min and eosin for 30 s, each followed by rinsing with tap water for 3 min. After the second rinsing step, the slides were immersed into 100% ethanol for 1 min and then in xylene. Cartilage tissue was stained using safranin-O for 2 min and Fast Green for 4 min with a short rinse in pure water in between. The stained sections were covered with a glass coverslip (Menzel Gläser, Braunschweig, Germany) using Entellan® mounting medium. After drying for 24 h, the stained sections were scanned with a Mirax Desk Scanner (Zeiss, Gottingen, Germany).

Calculation of gas-phase proton affinities

Gaussian 09[2] was used to calculate density functional theory energies and optimized geometries for neutral and protonated forms to determine the gas phase proton affinities of each of the individual drug compounds analyzed (refer to "single standard analysis" methods). Each structure was calculated using B3LYP/6-31G(2df,p), and all except those for paclitaxel were then also calculated using M06-2X/6-31G(2df,p). As each molecule typically has many protonation isomers (protomers), a variety of plausible sites for the proton were considered. However, it is possible that other energetically accessible protomers may have not been calculated. Frequency calculations were used to verify that

the structures were minima, and to calculate zero-point energies. The conformations that were calculated did not necessarily represent the global minimum, but the total energy difference arising from protonation is much greater than that separating different conformers. In each case, the lowest energy protomer was chosen to determine the proton affinity of the corresponding neutral molecule.

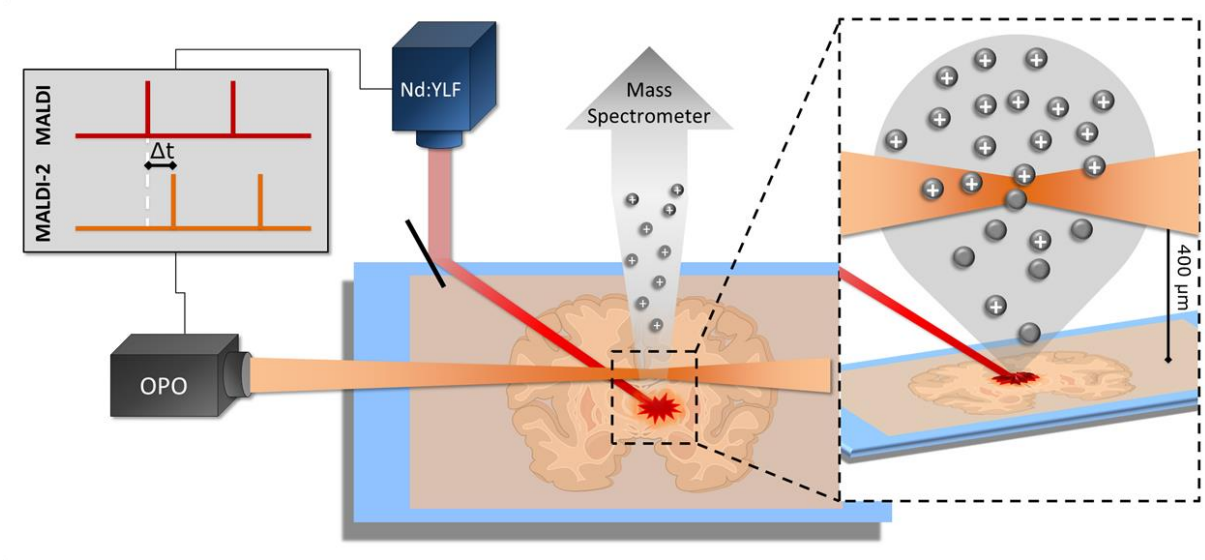

Supporting Information Figure 1. Post-ionization-MALDI (MALDI-2) set-up.

Compound	Molecular formula	Monoisotopic exact mass	Largest proton affinity (eV) B3LYP/6-31G(2df,p)	Largest proton affinity (eV) M062X/6-31G(2df,p)
caffeine	$C_8H_{10}N_4O_2$	194.0803	12.92	12.70
doxorubicine	$C_{27}H_{29}NO_{11}$	543.1740	10.54	10.25
fluoxetine	$C_{17}H_{18}F_3NO$	309.1340	9.95	9.84
haloperidol	$C_{21}H_{23}ClFNO_2$	375.1401	10.36	10.22
ibuprofen	$C_{13}H_{18}O_2$	206.1306	9.03	8.92
ketoconazole	$C_{26}H_{28}Cl_2N_4O_4$	530.1487	10.45	10.30
kynurenine	$C_{10}H_{12}N_2O_3$	208.0847	10.20	10.20
paclitaxel	$C_{47}H_{51}NO_{14}$	853.3309	10.22	NC
terfenadine	$C_{32}H_{41}NO_2$	471.3137	10.60	10.53
triamcinolone acetonide	$C_{24}H_{31}FO_6$	434.2104	9.80	9.79

Supporting Information Table 1. List of compounds with chemical formula, their monoisotopic exact mass, and highest gas-phase proton affinity values. (NC: Not Calculated)

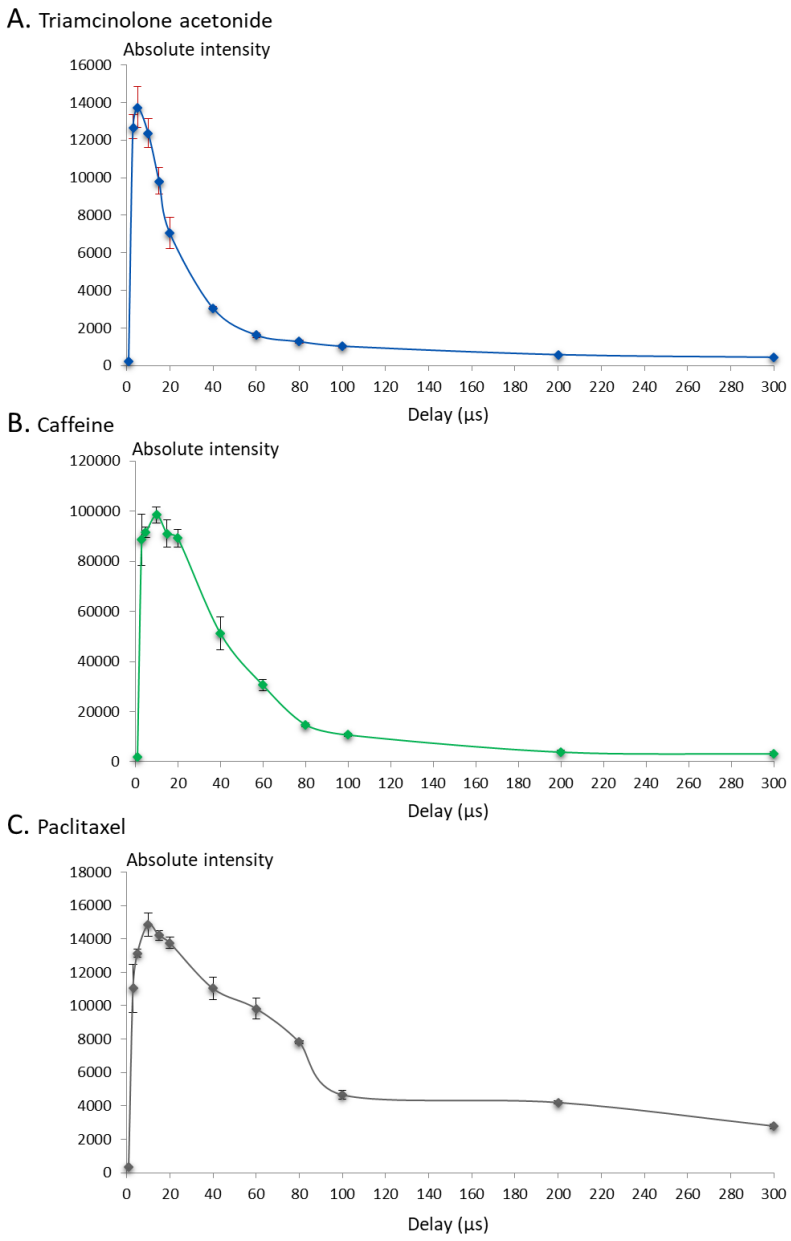

Supporting Information Figure 2. Post-ionization delay effects on protonated ion intensities from triamcinolone acetonide (**A**), caffeine (**B**), and paclitaxel (**C**) standards.

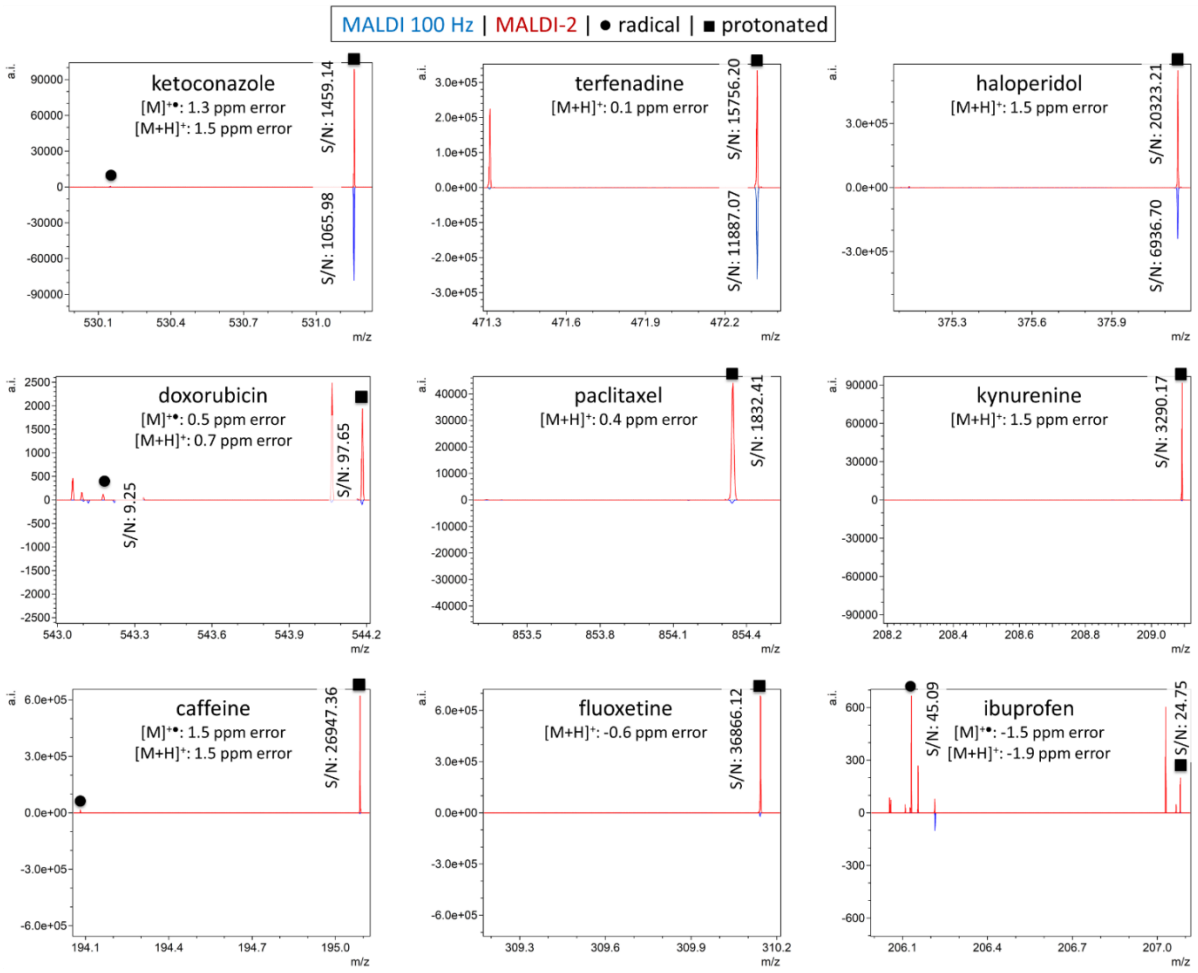

Supporting information Figure 3. Single-scan spectra from MALDI (blue) and MALDI-2 (red) showing the absolute intensity (a.i.) signal of the radical cations (●) and the protonated molecules (■) for every scanned compound. Signal-to-noise ratios are indicated S/N.

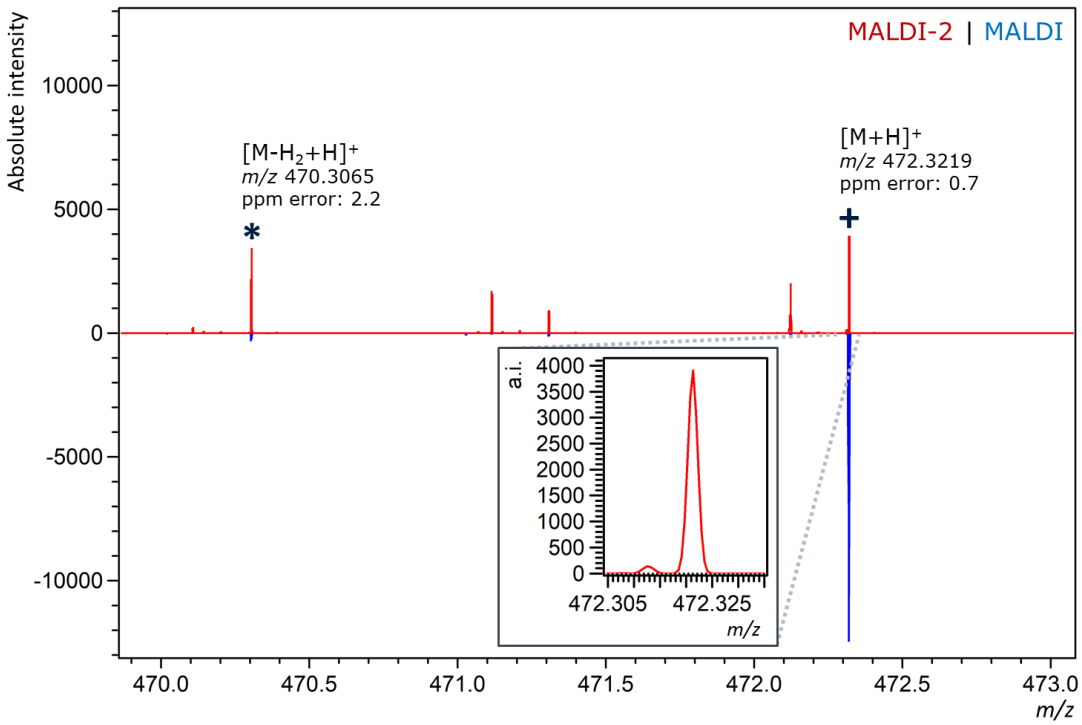

Supporting Information Figure 4. MALDI-2 (red) and MALDI (blue) spectra of terfenadine (0.001 mg/mL). MALDI-2 results in the formation of an abundant fragment ion at *m/z* 470.3065.

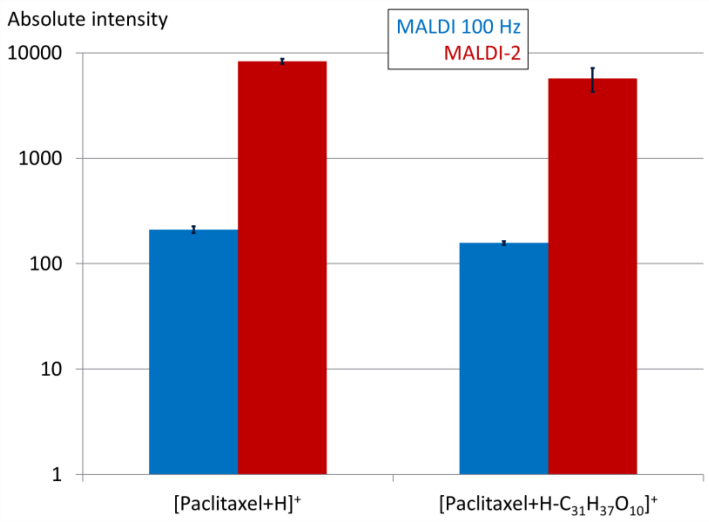

Supporting Information Figure 5. Absolute intensity comparison for paclitaxel (0.5 mg/mL) and its $[M+H-C_{31}H_{37}O_{10}]^+$ fragment generated by MALDI (blue) and MALDI-2 (red).

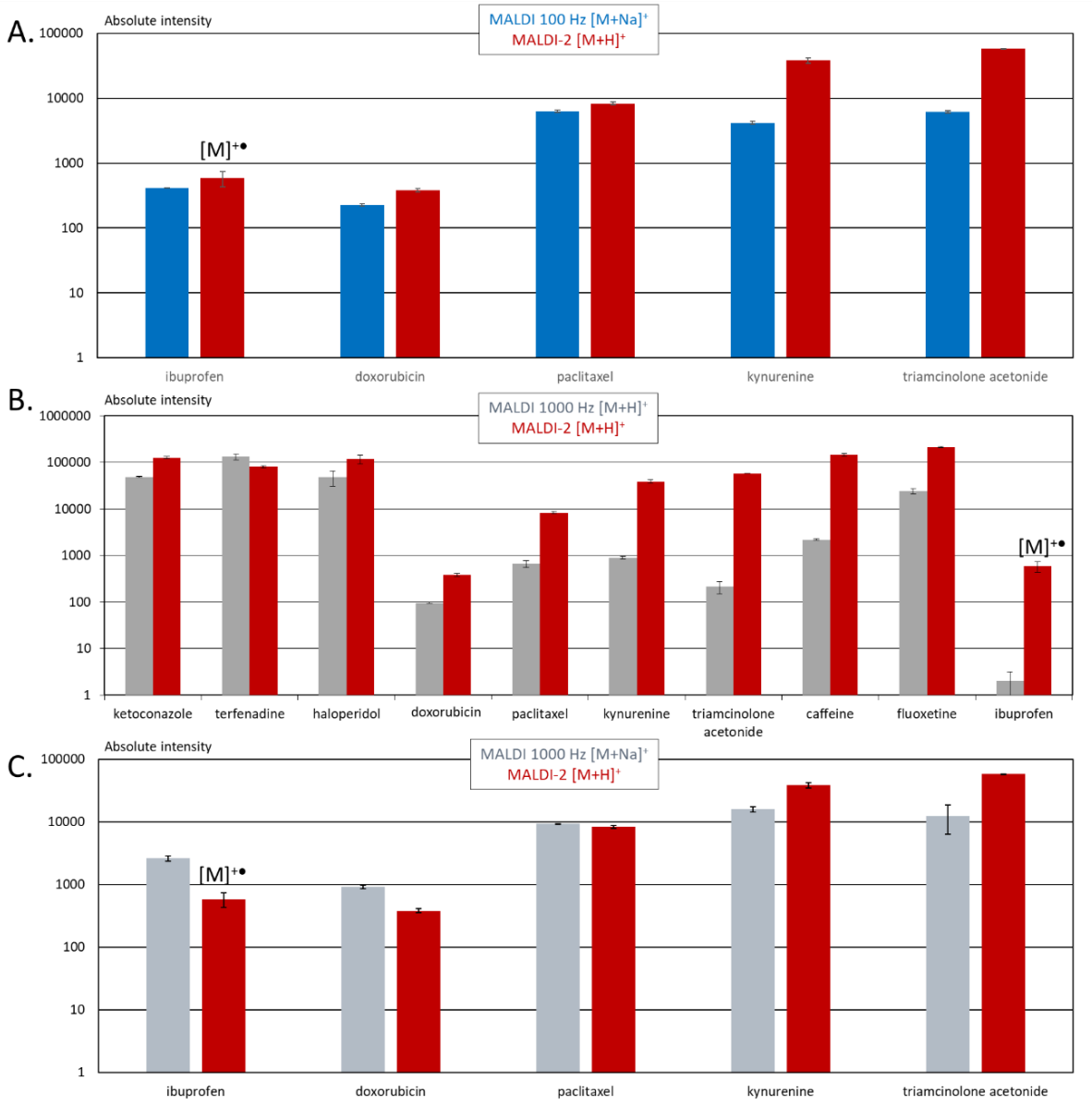

Supporting Information Figure 6. A. Comparison of the protonated signal (with the exception of ibuprofen [resented as the radical cation) for both MALDI (100 Hz; blue) and MALDI-2 (red). **B.** Comparison between MALDI (1000 Hz; grey) and MALDI-2 (red) only considering the protonated molecules for MALDI. **C.** Comparison between MALDI 1000 Hz and MALDI-2 considering the sodiated ions for MALDI. Note the logarithmic scale

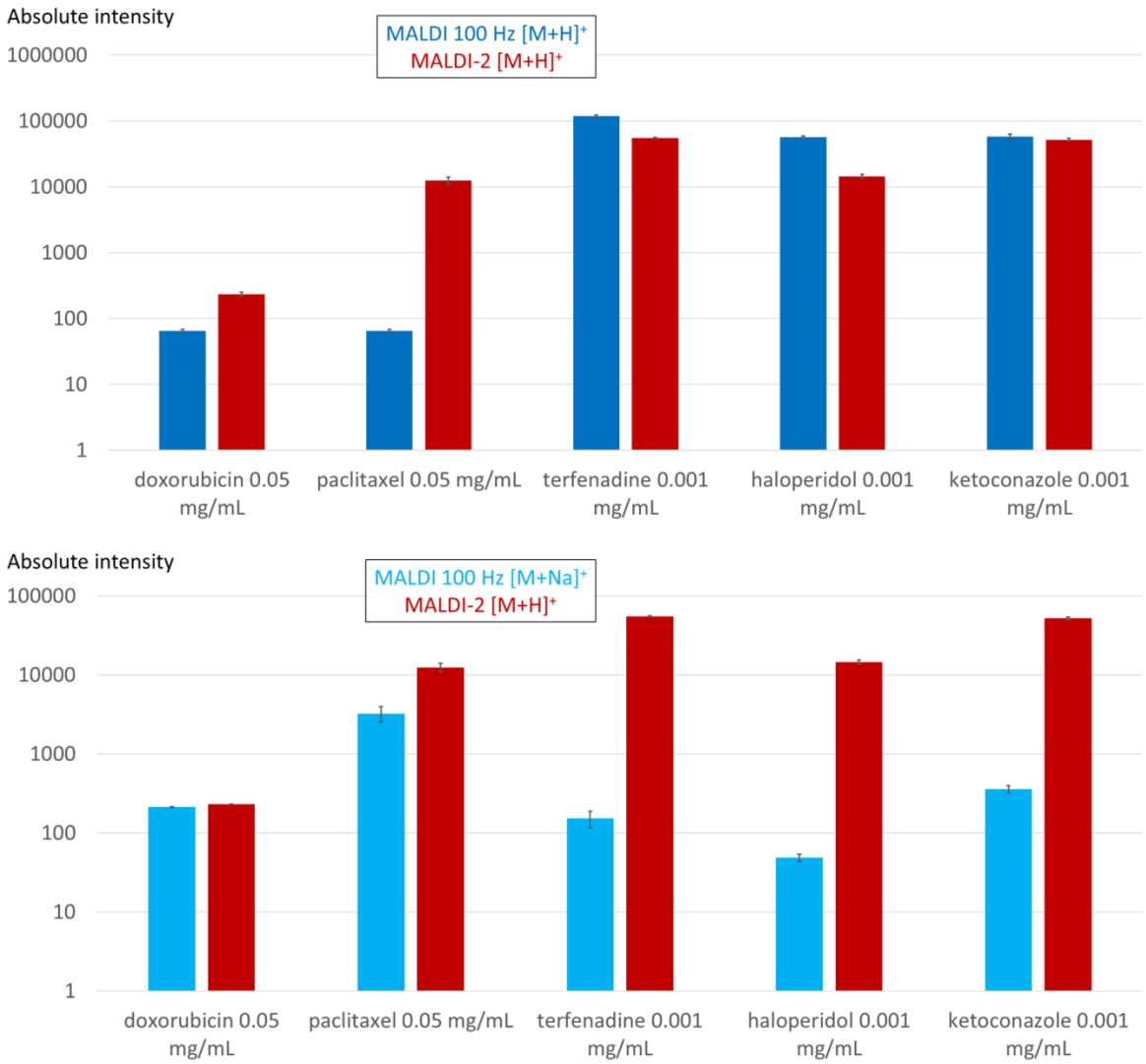

Supporting Information Figure 7. Absolute ion intensities of the protonated (top) and sodium (bottom) signals for doxorubicin (0.05 mg/mL), paclitaxel (0.05 mg/mL), terfenadine (0.001 mg/mL), ketoconazole (0.001 mg/mL), and haloperidol (0.001 mg/mL) acquired using MALDI (blue) and MALDI-2 (red).

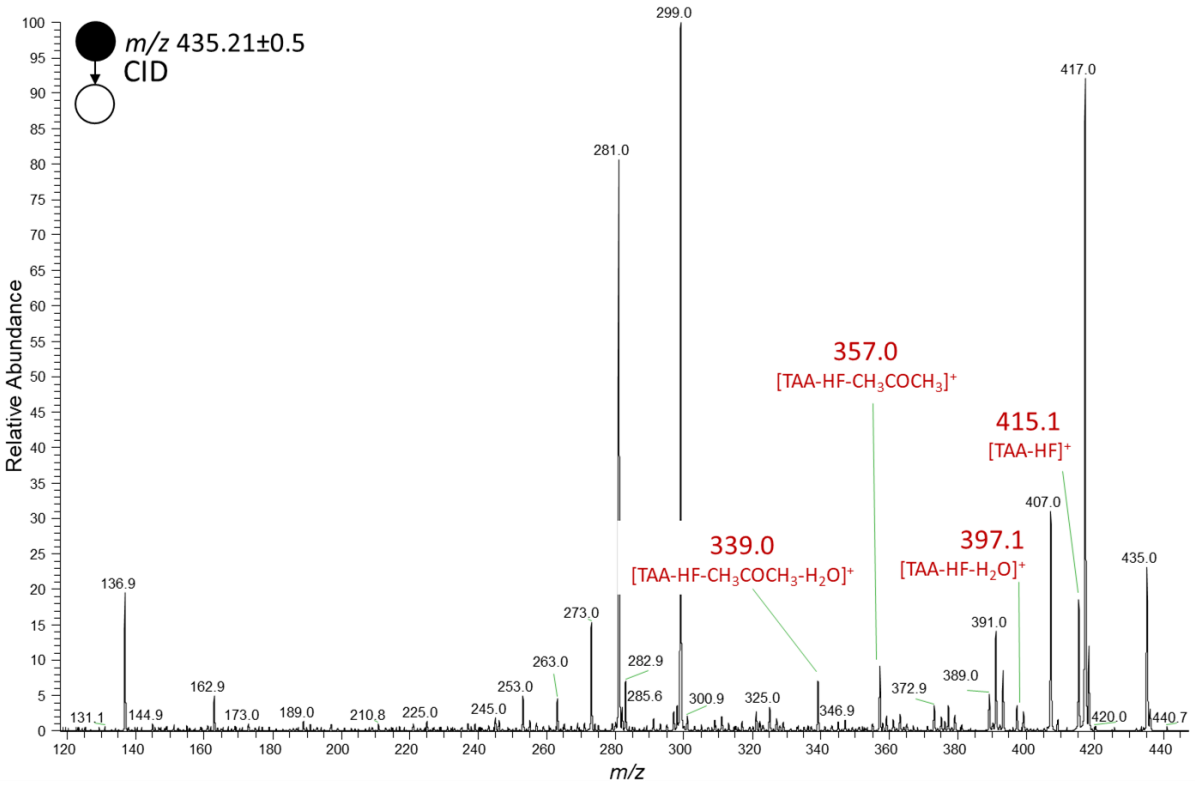

Supporting Information Figure 8. Low-energy CID MS/MS spectrum of the ions at *m/z* 435.21±0.5 detected from TAA dosed cartilage section in positive ion mode using the linear ion trap. Fragment ions supporting the assignment of TAA were found at *m/z* 339.0 ($[TAA\text{-}HF\text{-}CH_3COCH_3\text{-}H_2O]^+$), 357.0 ($[TAA\text{-}HF\text{-}CH_3COCH_3]^+$), 397.1 ($[TAA\text{-}HF\text{-}H_2O]^+$), and 415.1 ($[TAA\text{-}HF]^+$).

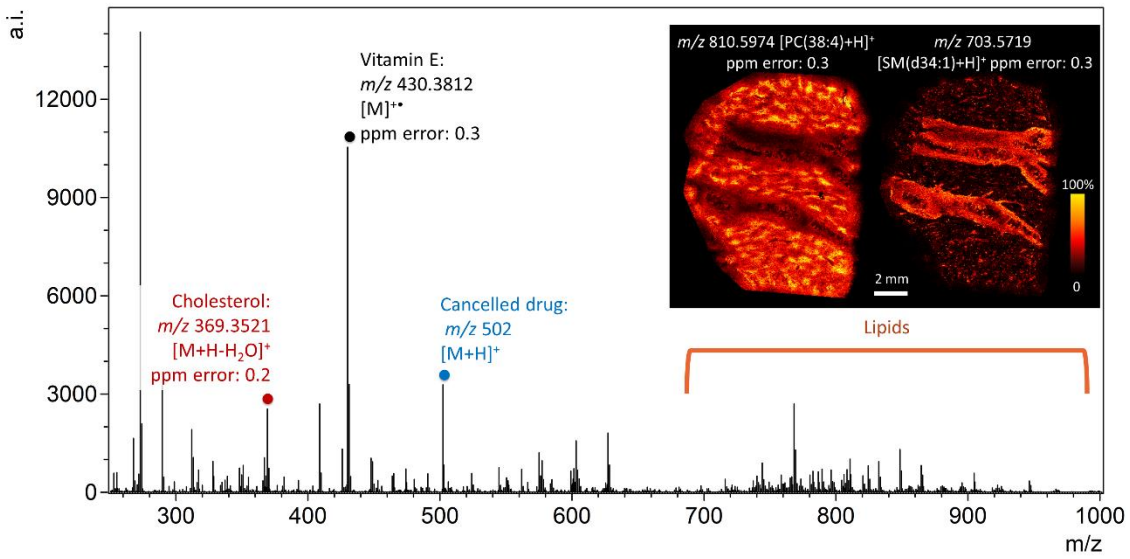

Supporting information Figure 9. Average spectrum obtained from dosed dog liver tissue using MALDI-2. Inset shows ion images for two endogenous lipid species. $[PC(38:4)+H]^+$ and $[SM(d34:1)+H]^+$. (a.i.: absolute intensity).

Caffeine Protonation Sites	
B3LYP/6-31G(2df,p)	eV
1	8.59
2	8.55
3	7.98
4	9.71
5	9.45
6	9.42
7	9.50
8	9.43
M062X/6-31G(2df,p)	eV
1	8.39
2	8.43
3	7.82
4	9.54
5	9.34
6	9.32
7	9.35
8	9.29

Doxorubicin Protonation Sites	
B3LYP/6-31G(2df,p)	eV
1	DNE
2	9.60
3	9.74
4	10.21
5	10.48
6	DNE
7	DNE
8	9.97
9	10.39
10	DNE
11	10.54
12	9.11
13	10.02
14	DNE
15	DNE
M062X/6-31G(2df,p)	eV
1	DNE
2	9.31
3	9.48
4	10.00
5	10.25
6	DNE
7	DNE
8	9.82
9	10.27
10	DNE
11	10.49
12	8.98
13	9.77
14	DNE
15	DNE

Fluoxetine Protonation Sites	
B3LYP/6-31G(2df,p)	eV
1	9.95
2	8.86
3	8.78
4	8.81
5	8.77
M062X/6-31G(2df,p)	eV
1	9.84
2	8.62
3	8.45
4	8.47
5	8.47

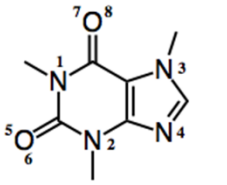

Caffeine

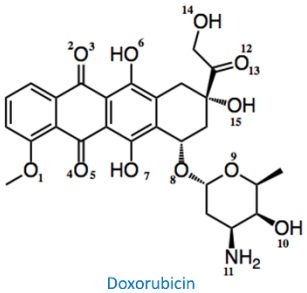

Doxorubicin

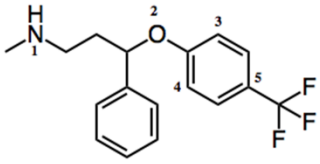

Fluoxetine

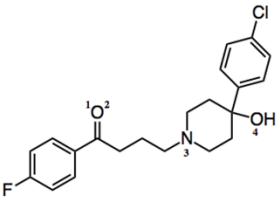

Haloperidol

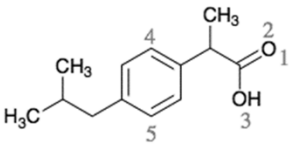

Ibuprofen

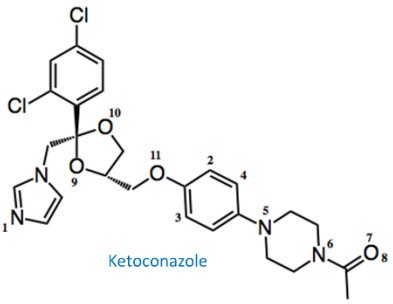

Ketoconazole

Haloperidol Protonation Sites	
B3LYP/6-31G(2df,p)	eV
1	9.28
2	9.38
3	10.36
4	DNE
M062X/6-31G(2df,p)	eV
1	9.00
2	9.15
3	10.22
4	DNE

Ibuprofen Protonation Sites	
B3LYP/6-31G(2df,p)	eV
1	8.67
2	9.03
3	DNE
4	8.70
5	8.71
M062X/6-31G(2df,p)	eV
1	8.54
2	8.92
3	DNE
4	8.33
5	8.37

Ketoconazole Protonation Sites	
B3LYP/6-31G(2df,p)	eV
1	10.45
2	9.04
3	9.44
4	9.39
5	9.96
6	9.23
7	9.61
8	9.72
9	8.57
10	8.60
11	DNE
M062X/6-31G(2df,p)	eV
1	10.30
2	8.68
3	9.21
4	9.29
5	9.82
6	9.12
7	9.52
8	9.63
9	8.39
10	8.39
11	DNE

*DNE = Does Not Exist

Supporting Information Figure 10. Proton affinity values of all compounds. Each structure was calculated using B3LYP/6-31G(2df,p), and all except those for paclitaxel were then also calculated using M06-2X/6-31G(2df,p).

Kynurenine Protonation Sites	
B3LYP/6-31G(2df,p)	eV
1	DNE
2	9.75
3	10.04
4	DNE
5	10.20
6	DNE
7	DNE
M062X/6-31G(2df,p)	eV
1	DNE
2	9.71
3	9.81
4	DNE
5	9.97
6	DNE
7	DNE

Paclitaxel Protonation Sites	
B3LYP/6-31G(2df,p)	eV
1	9.90
2	10.22
3	9.46
4	DNE
5	9.37
6	9.37
7	DNE
8	9.35
9	9.52
10	9.11
11	9.03
12	9.90
13	DNE
14	10.77
15	DNE
16	9.40
17	9.47
18	8.56
19	9.34
20	9.59
21	9.25

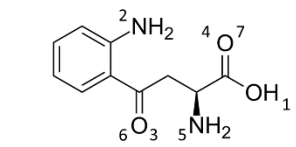

Kynurenine

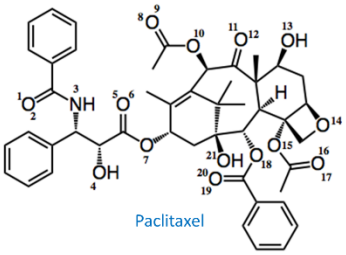

Paclitaxel

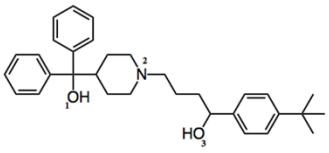

Terfenadine

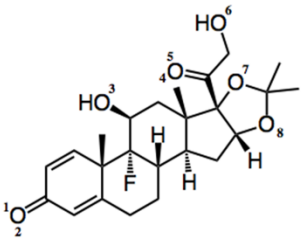

Triamcinolone acetonide

Terfenadine Protonation Sites	
B3LYP/6-31G(2df,p)	eV
1	9.82
2	10.60
3	DNE
M062X/6-31G(2df,p)	eV
1	DNE
2	10.53
3	DNE

Triamcinolone acetonide Protonation Sites	
B3LYP/6-31G(2df,p)	eV
1	10.06
2	10.06
3	8.37
4	8.74
5	9.13
6	DNE
7	DNE
8	8.61
M062X/6-31G(2df,p)	eV
1	9.79
2	9.80
3	8.14
4	8.52
5	8.91
6	DNE
7	DNE
8	8.38

*DNE = Does Not Exist

Supporting Information Figure 11. Proton affinity values of all compounds. Each structure was calculated using B3LYP/6-31G(2df,p), and all except those for paclitaxel were then also calculated using M06-2X/6-31G(2df,p).

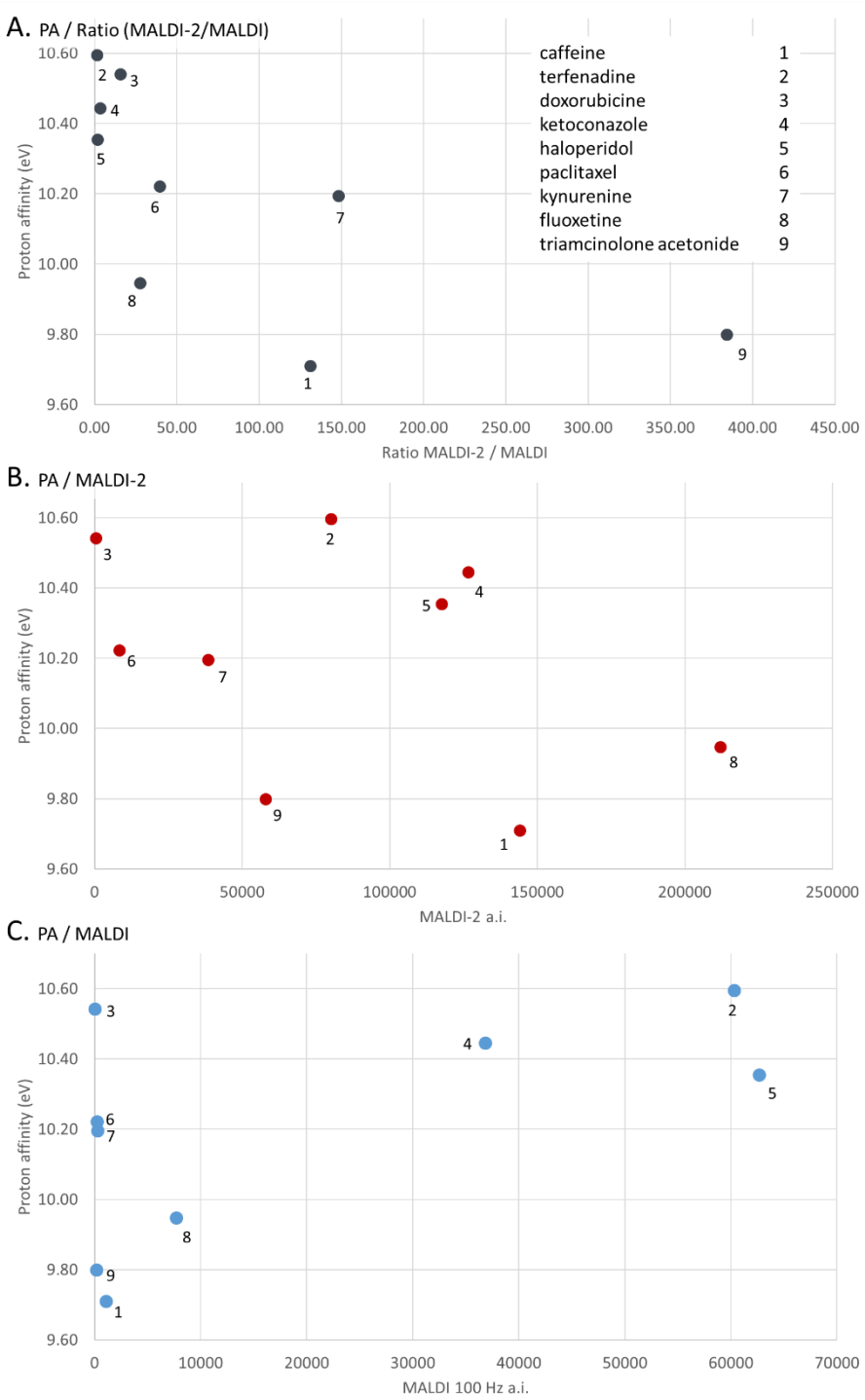

Supporting information Figure 12. A. Proton affinity (PA) values of all compounds plotted against (A) the MALDI2:MALDI ion intensity ratio for the corresponding $[M+H]^+$ ions, (B) $[M+H]^+$ ion intensity from MALDI-2 and (C) $[M+H]^+$ intensity from MALDI.

1 S. R. Ellis, J. Soltwisch, M. R. L. Paine, K. Dreisewerd, R. M. A. Heeren, *Chemical Communications* **2017**, *53*, 7246-7249 10.1039/c7cc02325a.
2 M. J. Frisch, G. W. Trucks, H. B. Schlegel, G. E. Scuseria, M. A. Robb, J. R. Cheeseman, G. Scalmani, V. Barone, G. A. Petersson, H. Nakatsuji, X. Li, M. Caricato, A. V. Marenich, J. Bloino, B. G. Janesko, R. Gomperts, B. Mennucci, H. P. Hratchian, J. V. Ortiz, A. F. Izmaylov, J. L. Sonnenberg, Williams, F. Ding, F. Lipparini, F. Egidi, J. Goings, B. Peng, A. Petrone, T. Henderson, D. Ranasinghe, V. G. Zakrzewski, J. Gao, N. Rega, G. Zheng, W. Liang, M. Hada, M. Ehara, K. Toyota, R. Fukuda, J. Hasegawa, M. Ishida, T. Nakajima, Y. Honda, O. Kitao, H. Nakai, T. Vreven, K. Throssell, J. A. Montgomery Jr., J. E. Peralta, F. Ogliaro, M. J. Bearpark, J. J. Heyd, E. N. Brothers, K. N. Kudin, V. N. Staroverov, T. A. Keith, R. Kobayashi, J. Normand, K. Raghavachari, A. P. Rendell, J. C. Burant, S. S. Iyengar, J. Tomasi, M. Cossi, J. M. Millam, M. Klene, C. Adamo, R. Cammi, J. W. Ochterski, R. L. Martin, K. Morokuma, O. Farkas, J. B. Foresman, D. J. Fox, Gaussian 09 Rev. E.01, Wallingford, CT, **2016**.